doi.org/10.62683/SINARG2025.174

Research paper

DIMENSIONING OF STRUTS FOR REINFORCED CONCRETE DIAPHRAGM WALLS TO SECURE EXCAVATION OF ADJACENT STRUCTURES

Radovan Perić[1], Dragana Turnić[2], Marija Spasojević Šurdilović[3], Srđan Živković[4]

Abstract:

Modern architectural solutions in densely populated areas require structures with multiple underground levels. With advancements in construction technology, numerous solutions have been developed to secure the excavation of foundation pits and adjacent structures. The most rational solution adopted is the securing of the excavation and adjacent structures with reinforced concrete diaphragm walls supported by steel struts at two levels. The paper outlines the specifics of the structural solution, with a detailed analysis of the steel struts. Special emphasis is placed on the stability control of the struts, which was conducted using various methods outlined in Eurocode 3. The control of flexural buckling was performed through the application of the equivalent column method, the use of equivalent geometric imperfections, and the implementation of both geometrically and materially nonlinear analysis with imperfections.

Key words: *Stability, Flexural Buckling, Eccentric Compression, Equivalent Column Method, Reinforced Concrete Diaphragm Walls*

[1]MSc, Teaching Associate, Faculty of Civil Engineering and Architecture, University of Niš, Serbia,radovan.peric@gaf.ni.ac.rs, ORCID 0009-0003-3022-7898
[2]PhD, Associate Professor, Faculty of Civil Engineering and Architecture, University of Niš, Serbia, dragana.turnic@gaf.ni.ac.rs, ORCID 0000-0001-7494-8257
[3]PhD, Associate Professor, Faculty of Civil Engineering and Architecture, University of Niš, Serbia, marija.spasojevic.surdilovic@gaf.ni.ac.rs, ORCID 0000-0003-3376-1909
[4]PhD, Full Profesor, Faculty of Civil Engineering and Architecture, University of Niš, Serbia, srdjan.zivkovic@gaf.ni.ac.rs, ORCID 0000-0002-7726-4149

1. INTRODUCTION

In contemporary urban environments, modern architectural solutions increasingly demand the construction of buildings with multiple underground levels, especially in densely populated areas. These conditions present significant challenges in both structural stability and excavation safety. At the same time, the advancement of construction technologies has enabled the implementation of efficient and reliable methods for deep excavation and soil retention. Among these, the use of reinforced concrete diaphragm walls, installed along the excavation perimeter and supported by steel struts at multiple levels, has emerged as one of the most rational and widely adopted solutions for safeguarding both the construction site and neighboring structures.

Diaphragm walls with strut supports represent a structural-retention system that combines load-bearing walls with additional elements, typically steel struts, designed to improve load distribution and increase resistance to lateral earth pressures. These systems are commonly employed in both residential and commercial developments, as well as in specialized civil engineering projects where high safety standards and long-term performance are essential.

This paper will examine the fundamental characteristics of reinforced concrete diaphragm walls with strut supports, the principles of strutanalysis and design, as well as the theoretical background related to structural instability. Additionally, a practical case study will be presented alongside a numerical model of the strut system, which will serve as the basis for a parametric analysis.

2. THEORETICAL BACKGROUND AND PREVIOUS RESEARCH

The problem of flexural buckling of an axially compressed member within the elastic range was first addressed by Leonhard Euler in 1744. The fundamental assumptions underlying Euler's theory of linear elastic buckling are as follows:

- the material is homogeneous, isotropic, and behaves in a linearly elastic manner;
- the member is perfectly straight, with no geometric imperfections;
- both ends of the member are pinned (hinged) supports;
- the member is subjected to concentrically axial forces at its ends;
- the cross-section is constant and monolithic along the member's length;
- torsional deformations are fully restrained.

In addition to the previously stated assumptions, it is also considered that the curve describing the relationship between axial force and lateral deflection is bilinear. As long as the applied axial force remains below the critical value ($N_{ed} < N_{cr}$), no deflection occurs. Upon reaching the critical force, buckling initiates and deformations tend toward infinity, which characterizes the phenomenon of bifurcation instability.

The differential equation of the elastic curve is a homogeneous differential equation with constant coefficients, expressed as:

$$v'' + k^2 v = 0 \tag{1}$$

Solving this equation yields the expression for the minimum value of the critical force:

$$F = \frac{\pi^2}{L_i^2} EI = N_{cr} \tag{2}$$

where:

- *v* is the lateral deflection of the member,
- *k* is a constant related to the buckling mode,
- *EI* is the flexural rigidity of the member,
- *F* is the axial force applied at the ends of the member,
- L_i is the effective buckling length of the member.

The given expression defines the buckling behavior of a column within the elastic domain, valid as long as the critical buckling stress does not exceed the proportional limit of the material from which the column is made. The corresponding slenderness ratio at the proportional limit, denoted as λ_p serves as a clear boundary between the elastic and plastic domains. This limit is defined by the following expression:

$$\lambda_p = \pi \sqrt{\frac{E}{235}} \varepsilon \tag{3}$$

The expression provided by equation (2) can be applied to columns with slenderness ratios greater than λ_p. In such cases, the problem is purely geometrically nonlinear, while the material remains within the elastic range.

Since real structural elements in civil engineering are often characterized by relatively low slenderness, it becomes necessary to introduce material nonlinearity into the analysis. Numerous researchers, including Tetmajer, von Kármán, Engesser, Shanley, and others, have sought to develop more accurate σ–λ relationships in the plastic domain by accounting for the variability of compressive force during the process of stability loss.

Starting from the differential equation derived from equilibrium conditions for an axially loaded column with initial geometric imperfections:

$$v'' + k^2 v = -k^2 \delta_0 \sin\left(\pi \frac{x}{L}\right) \tag{4}$$

and assuming boundary conditions corresponding to a column pinned at both ends (first buckling mode), the critical force is obtained using Equation (2). The total mid-span deflection of the column is given by:

$$\delta_{tot} = \delta_0 \frac{1}{1 - \frac{N}{N_{cr}}} \tag{5}$$

Assuming that the column remains in the elastic domain, the following condition must be satisfied:

$$\frac{N_u}{A} + \frac{N_u \cdot \delta_{tot}}{W} \leq f_y \tag{6}$$

Introducing the dimensionless parameters defined as:

$$\eta = \frac{\delta_0 \cdot A}{W}, \ \chi = \frac{N_u}{N_{pl}}, \bar{\lambda} = \sqrt{\frac{N_{pl}}{N_c}} \tag{7}$$

leads to the Ayrton–Perry function, which forms the basis of modern design standards:

$$\chi^2\bar{\lambda}^2 - \chi(1+\eta+\bar{\lambda}^2) + 1 = 0 \quad (8)$$

Solving this quadratic equation under the condition of real solutions yields the general expression for the nondimensional buckling reduction factor χ:

$$\chi = \frac{1}{\Phi+\sqrt{\Phi^2-\bar{\lambda}^2}} \quad (9)$$

where:

- δ_0– initial geometric imperfection,
- δ_{tot} – total mid-span deflection,
- N_u– ultimate buckling force,
- A – cross-sectional area,
- f_y – yield strength of the material,
- W – elastic section modulus,
- χ – nondimensional buckling reduction factor,
- $\bar{\lambda}$– relative (nondimensional) slenderness for the considered buckling axis,
- η – auxiliary coefficient,
- Φ – auxiliary coefficient dependent on the imperfection factor α for European buckling curves.

In addition to the method based on European buckling curves i.e., the equivalent column method, Eurocode also allows for stability verification using the initial geometric imperfection method. For elastic global analysis, the equivalent geometric imperfection for a specific case is taken as L / 200, and the failure criterion is defined by stresses calculated according to second-order theory. In addition to flexural buckling, eccentric compression must also be checked, as noted in [1], while local buckling effects are not explicitly considered. Structural safety with respect to local instability is ensured by selecting an appropriate cross-section class.

2.1. Influence of Imperfections

The critical axial force calculated using Equation (2) is approximately three times higher than the actual buckling load observed in practice. This discrepancy arises primarily due to material and geometric imperfections. Common material imperfections include residual stresses and variations in the mechanical properties of the material, such as yield strength and modulus of elasticity. Geometric imperfections typically include cross-sectional irregularities, initial curvature or deviation of the member axis from straightness, and load eccentricity.

To address these factors, a wide range of deterministic and stochastic methods for sensitivity and uncertainty analysis have been developed [2]. The deterministic approach relies on parametric analysis, where the influence of a single varying parameter on the result is examined. In contrast, stochastic methods provide a better understanding of the influence of variable parameters by offering insights into standard deviation, mean deviation, and other statistical measures.

Vrednost faktora amplifikacije zavisi od više faktora, ali ukazuje na to da krajnje odsupanje ose štapa može biti do četiri puta veće od početne geometrijske imperfekcije [3].

The value of the amplification factor depends on several parameters, but it indicates that the final deviation of the member axis can be up to four times greater than the initial geometric imperfection [3]. Initial geometric imperfections are influenced by various factors, among

which material quality, manufacturing process, and surface finishing techniques are among the most significant. The material from which the profiles are made plays a major role in determining the magnitude of these initial imperfections.

Testing of 24 specimens revealed deviations ranging from L/756 to L/23,605, with an average value of L/5,805, indicating that profiles made of high-strength steel (HSS) exhibit significantly smaller initial imperfections. When applying the buckling curves provided in [1], conservative results are obtained, with a deviation of approximately 33% [4], highlighting the conservative nature of the current design code when sizing members fabricated from high-strength steel (HSS). The manufacturing process has a significant influence not only on residual stresses, but also on geometric imperfections. The adverse effects of production-related imperfections can be minimized through the use of HSS, as confirmed by the experimental results presented in [5]. The influence of welding and surface finishing does not play a dominant role in the occurrence of either local or global buckling in steel grade S355, as indicated in [6]. Spirally welded steel pipes are increasingly used in the construction industry due to the possibility of producing pipes in greater lengths and achieving optimal diameter-to-wall-thickness ratios. Previous studies have primarily focused on their application in linear infrastructure projects, such as oil pipelines, excavation support systems in combination with Larsen sheet piles, and in cased piles [7].

The imperfections in these profiles largely depend on the welding method. Welding can induce significant residual stresses, and weld shrinkage can result in local geometric imperfections [8]. These initial local imperfections are considered the primary cause of stability loss in spirally welded pipes [9], [10], [11]. Longitudinal deformation can lead to cross-sectional ovalization, a phenomenon also known as the Brazier effect. Ovalization reduces the pipe's bending stiffness due to flattening, increases the local cross-sectional radius in regions of highest compression, and introduces biaxial stress states due to ring bending, ultimately leading to premature failure of the pipe.

As bending deformation increases, structural instability may arise in the compressed region of the pipe in the form of local buckling, commonly referred to as "local buckle," "wrinkle," or "kink." Pipes with D/t ratios below 70 exhibit a gradual development of local instability, and collapse is not as sudden as in pipes with higher D/t ratios.

The welding method used in the fabrication of spirally welded pipes significantly affects the distribution of residual stresses. Longitudinal residual stresses influence the load-bearing capacity, fatigue performance, brittle fracture resistance, and stress corrosion cracking, with these effects being particularly pronounced in moderately slender pipes [12], [13], [14]. Due to the high production cost of hot-rolled pipes, they are typically used in installations that require fluid-tightness. As a result of their manufacturing process, hot-rolled pipes exhibit a more favorable residual stress distribution and lower initial geometric imperfections. Comparative analyses between cold-formed and hot-rolled profiles indicate that cold-formed profiles deliver satisfactory performance, especially when their significantly lower production costs are considered [15].

The ultimate strength and ductility of a profile depend heavily on its buckling resistance. Local buckling of a single member can critically affect the overall behavior of the structural system [16]. In order to minimize the risk of catastrophic failure, numerous researchers have proposed modifications to the Eurocode buckling curves [17].

3. CASE STUDY OF A STRUT SYSTEM MODEL FROM PRACTICE

The planned commercial building (2Bas+Gr+8) is located in Belgrade, cadastral municipality of Dorćol, and is surrounded by neighboring structures with heights of Gr+9 and Bas+5. The proximity of the Danube River influences the groundwater level, which varies with river stages and ranges from 2.60 m to 5.50 m relative to the ground floor elevation. Based on geotechnical field and laboratory investigations, the soil profile has been identified as Danube alluvium, predominantly composed of highly permeable sandy soil.

As the optimal solution for securing the excavation of the foundation pit and protecting adjacent structures, reinforced concrete diaphragm walls with a thickness of 60 cm (locally increased to 80 cm) were adopted. The diaphragm wall thickness was determined by the location of the regulatory boundary line and the dimensions of the newly designed building. Due to a foundation depth of 14.20 m, the construction is planned to be executed in phases, with two levels of strut support. The struts are nominally pinned at both ends and are primarily subjected to axial compressive forces. An axonometric view of the strut layout is shown in Figure 1.

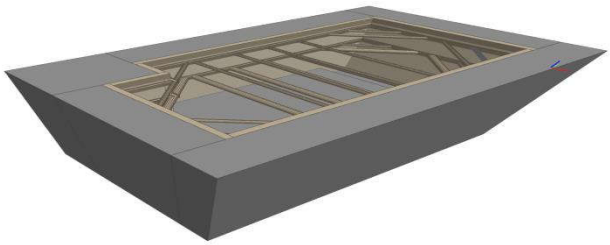

Figure 1. Axonometric view of the strut support system for the foundation pit

The struts span 16.50 meters and are subjected to high-intensity axial compressive forces, which lead to buckling. They are fabricated from spirally welded, cold-formed steel pipes with a diameter of 800 mm and a wall thickness of 16 mm. In the event of strut instability, a global loss of stability of the entire retaining system, as well as damage to adjacent structures, may occur. This highlights the need for a detailed limit state analysis. The stability of these elements is significantly influenced by the initial geometric imperfection [2].

According to national standards, the initial out-of-straightness must not exceed a limit value of L / 1000 [18], [19]. However, field inspections of completed structures have revealed initial curvatures that exceed these limits, which may result from excessive initial curvature, localized overloading, construction errors, or other unforeseen factors [3]. Due to geometric nonlinearity, the amplitude of initial curvature may amplify, ultimately leading to loss of stability. When the initial imperfection exceeds L / 1000, the load-bearing capacity can no longer be verified using current design codes. Moreover, the relationship between initial curvature and axial capacity is nonlinear and influenced by multiple factors, such as member slenderness and residual stresses, which must be carefully considered [4], [6].

4. NUMERICAL MODEL

To better evaluate the influence of geometric imperfections, this study includes a parametric analysis of the effects of initial geometric imperfections. The static system of the analyzed strut is modeled as a simply supported beam. The strut connections are idealized as pinned joints, incapable of transferring bending moments. The load transferred through

the reinforced concrete diaphragm is considered centrically applied, and diaphragm rotation during strut instability is neglected.

The values of initial imperfections are adopted based on experimental results from [3] and [20], as well as from construction tolerance limits defined in [18], ranging from L/2000 to L/75. The self-weight of the strut is included in the analysis due to its impact on initial imperfections. Initial geometric imperfections were modeled as half sine waves with varying amplitudes, as shown in Table 1. Material imperfections are not considered in this study.

Table 1. Initial Geometric Imperfections

n	3000	2000	1900	1800	1700	1600	1500	1400	1300	1200	1100
δ_0	10.10	12.85	13.29	13.77	14.31	14.92	15.60	16.39	17.29	18.35	19.60
n	1000	900	800	700	600	500	400	300	200	100	75
δ_0	21.10	22.94	25.23	28.17	32.10	37.60	45.85	59.60	87.10	169.6	224.6
The initial imperfection is represented as L/n δ_0- Initial imperfection with corresponding deflection impact [mm]											

The numerical analysis was carried out using the FEM software package Femap with NX Nastran v12.00, applying the finite element method [21]. The element size was determined through a convergence study, which showed that accurate results are achieved when the beam is divided into 18 finite elements. Modeling was performed using beam-type finite elements. The structural analysis was conducted using GMNIA (Geometrically and Materially Nonlinear Analysis with Imperfections).

Material nonlinearity was modeled with an elastic–perfectly plastic stress–strain relationship, without strain hardening, using a yield strength of 235 MPa. A geometrically nonlinear analysis was performed using 100 load increments, with displacement-based convergence via the Full Newton-Raphson method. The corresponding stress distribution is shown in Figure 2.

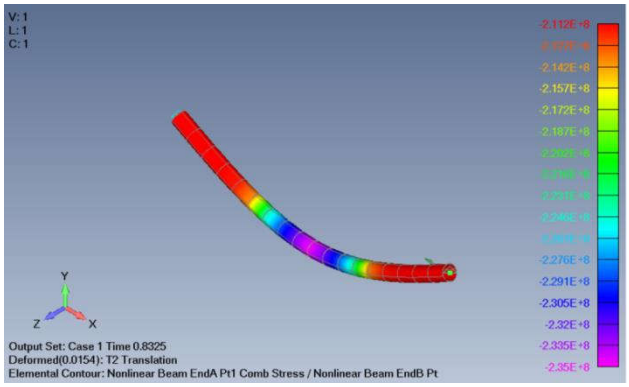

Figure 2. Representation of the element at critical load for L/1000 imperfection

5. RESULTS AND DISCUSSION

To investigate the influence of initial geometric imperfections on the critical force leading to global stability loss, a total of 22 numerical models were analyzed. The results are presented in Table 2.

Table 2. Critical buckling force

n	3000	2000	1900	1800	1700	1600	1500	1400	1300	1200	1100
N_{cr}	8769	8653	8631	8613	8591	8566	8538	8506	8469	8428	8381
n	1000	900	800	700	600	500	400	300	200	100	75
N_{cr}	8325	8256	8175	8075	7944	7775	7538	7184	6600	5394	4847
The initial imperfection is represented as L/n N_{cr} –critical force causing buckling [kN]											

To facilitate interpretation of the results and to observe the trend in the variation of the critical force as a function of the initial geometric imperfection, the results are presented graphically in Figure 3. The analysis reveals that the critical buckling force decreases sharply for initial geometric imperfections exceeding L/600.

The critical buckling force obtained using Equation (2) is 23060 kN, while the axial load-bearing capacity of the cross-section under concentric compression, as per [1], is 9260.91 kN. When comparing this value to the critical force corresponding to an initial geometric imperfection of L/3000, it can be observed that such a small imperfection has minimal influence on the overall load-bearing capacity.

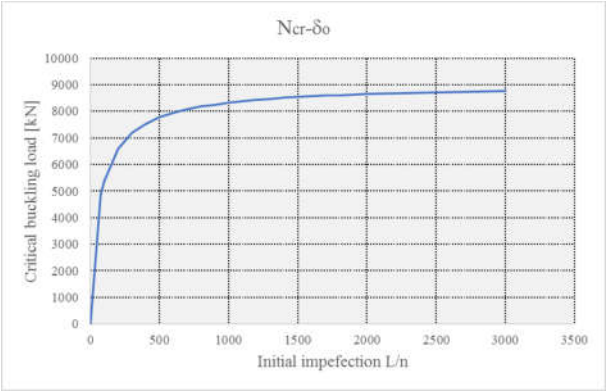

Figure 3. Relationship between critical force and initial geometric imperfection

The flexural buckling capacity, calculated using the equivalent column method in accordance with Eurocode, is 7084 kN, which closely corresponds to an initial imperfection of L/300. The bending moments induced in the member are of low intensity, and their contribution to global stability loss is minor. The results of the eccentric compression check also align with the imperfection value of L/300.

According to [2], the permissible deviation of a structural member from the ideal straight line is L/1000. Numerical analysis yielded a critical force of 8325 kN, at which a lateral deflection of 15.4 mm occurs. The corresponding stress distribution is shown in Figure 5.

The presented results indicate that Eurocode provides conservative estimates, with a deviation of approximately 17.5%, which is consistent with the findings reported in [3].

6. CONCLUSION

This study investigated the stability of excavation struts for the foundation pit of a newly designed structure, considering various initial geometric imperfections. The axial load capacity of the strut members was evaluated as a function of initial imperfection using both

analytical and numerical methods. A geometrically and materially nonlinear analysis with imperfections (GMNIA) was conducted using the finite element method. The theoretical background of the applied methods, types of structural instability, key equations, and strength criteria were presented.

A parametric analysis was used to assess the sensitivity of the critical buckling force to initial geometric imperfections. The GMNIA results yielded slightly higher critical forces compared to those calculated in accordance with Eurocode. The rational application of Eurocode design provisions could be improved through modifications to the current buckling curves.

When analyzing reinforced concrete diaphragm walls supported by struts, proper dimensioning of the struts is of crucial importance. GMNIA provides a more realistic representation of stress states, deformations, and displacements under various load levels, enabling more efficient and reliable design of both struts and diaphragm walls. A significant impact of initial geometric imperfections was observed for values greater than L/600.

Further research could include the influence of material nonlinearity, particularly the effects of residual stresses. Given the increasing use of spirally welded pipes due to their cost-effectiveness, it would be beneficial to explore their application in conventional engineering structures. Additionally, since boundary conditions significantly affect the critical buckling force, where a fully fixed strut exhibits up to four times higher capacity than a pinned one, the influence of semi-rigid connections remains a promising direction for future investigation.

ACKNOWLEDGMENTS

This research was supported by the Ministry of Science, Technological Development and Innovation of the Republic of Serbia under the Agreement on the Implementation and Financing of Scientific Research Work of the NIO in 2025 - Registration number: 451-03-136/2025-03/ 200095 dated 04/02/2025.

REFERENCES

[1] Institut za standardizaciju Srbije: **SRPS EN 1993-1-1 – Projektovanje čeličnih konstrukcija - Deo 1-1: Opšta pravila i pravila za zgrade**, Beograd, 2012.

[2] Kala Zdeněk: **Sensitivity assessment of steel members under compression.** *Engineering Structures*, Vol. 31, No. x, pp. 1344–1348, 2009, doi:10.1016/j.engstruct.2008.04.001.

[3] Yang Xu, Xiang Yang, Luo Yong-Feng, Guo Xiao-Nong, Liu Jun: **Axial compression capacity of steel circular tube with large initial curvature: Column curve and application in structural assessment.** *Journal of Constructional Steel Research*, Vol. 177, 2021, https://doi.org/10.1016/j.jcsr.2020.106481.

[4] Shi Gang, Jiang Xue, Zhou Wenjing, Chan Tak-Ming, Zhang Yong: **Experimental study on column buckling of 420 MPa high strength steel welded circular tubes.** *Journal of Constructional Steel Research*, Vol. 100, 2014, pp. 71–81, http://dx.doi.org/10.1016/j.jcsr.2014.04.028.

[5] Fan Feng, Yan Jiachuan, Cao Zhenggang: **Elasto-plastic stability of single-layer reticulated domes with initial curvature of members.** *Thin-Walled Structures*, Vol. 60, 2012, pp. 239–246, http://dx.doi.org/10.1016/j.tws.2012.01.012.

[6] Szafran Jacek, Kamiński Marcin, Juszczyk-Andraszyk Klaudia: **Steel hot-rolled, cold-formed, and hot-finished structural hollow section – an experimental stability study.** *Lightweight Structures in Civil Engineering,* XXII LSCE, 2016.

[7] Jaya Angelina, Myers Andrew, Torabian Shahabeddin, Mahmoud Abdullah, Smith Eric, Agbayani Nestor, Schafer Ben: **Spirally welded steel wind towers: Buckling experiments, analyses, and research needs.** *Journal of Constructional Steel Research,* Vol. 125, 2016, pp. 218–226, http://dx.doi.org/10.1016/j.jcsr.2016.06.022.

[8] Farhad Aslani, Uy Brian, Hicks Stephen, Kang Won-Hee: **Spiral welded tubes – imperfections, residual stresses, and buckling characteristics.** *Advances in Steel Structures*, Lisbon, Portugal, July 22–24, 2015. DOI:10.13140/RG.2.1.1399.7927/2

[9] Jay Angelina, Mirzaie Fariborz, Myers Andrew, Torabian Shahabeddin, Mahmoud Abdullah, Smith Eric, Schafer Benjamin: **The Effect of Geometric Imperfections on the Flexural Buckling Strength of Tapered Spirally Welded Steel Tubes.** *Proceedings of the Annual Stability Conference, Structural Stability Research Council*, Orlando, Florida, April 12–15, 2016,

[10] Zimmerman Tom, Timms Chris, Xie Jueren, Asante James: **Buckling resistance of large diameter spiral welded line pipe**. *International Pipeline Conference*, Canada, Alberta, October 4–8, 2024.

[11] Van Es Sjors, Gresnigt Arnold, Vasilikis Daniel, Karamanos Spyros: **Ultimate bending capacity of spiral-welded steel tubes – Part I: Experiments.** *Thin-Walled Structures*, Vol. 102, 2016, pp. 286–304, http://dx.doi.org/10.1016/j.tws.2015.11.024.

[12] Huang Yuner, Young Ben: **Design of cold-formed stainless steel circular hollow section columns using direct strength method.** *Engineering Structures,* Vol. 163, 2018, pp. 177–183, https://doi.org/10.1016/j.engstruct.2018.02.012.

[13] Puthli Ram, Packer Jeffrey: **Structural design using cold-formed hollow sections.** *Steel Construction,* Vol. 6, No. 2, 2013, DOI:10.1002/stco.201310013.

[14] Xu Yan, Zhang Mingyu, Zheng Baofeng: **Design of cold-formed stainless steel circular hollow section columns using machine learning methods.** *Structures,* Vol. 33, 2021, pp. 2755–2770, https://doi.org/10.1016/j.istruc.2021.06.030.

[15] Yang Chang, Zhao Hua, Sun Yuping, Zhao Shichun: **Compressive stress-strain model of cold-formed circular hollow section stub columns considering local buckling.** *Thin-Walled Structures,* Vol. 120, 2017, pp. 495–505, http://dx.doi.org/10.1016/j.tws.2017.09.017.

[16] Yan Xi-Feng, Yan Chao: **Experimental research and analysis on residual stress distribution of circular steel tubes with different processing techniques.** *Thin-Walled Structures*, Vol. 144, 2019, 106268, https://doi.org/10.1016/j.tws.2019.106268.

[17] Shi Gang, Jiang Xue, Zhou Wenjing, Chan Tak-Ming, Zhang Yong: **Experimental Investigation and Modeling on Residual Stress of Welded Steel Circular Tubes.** *International Journal of Steel Structures,* Vol. 13, No. 3, 2013, pp. 495–508, DOI:10.1007/s13296-013-3009-y.

[18] Institut za standardizaciju Srbije: **SRPS EN 1090-2:2024 – Izvođenje čeličnih i aluminijumskih konstrukcija – Deo 2: Tehnički zahtevi za čelične konstrukcije.** Beograd, 2024.

[19] Institut za standardizaciju Srbije: **SRPS EN ISO 13920 – Zavarivanje – Opšte tolerancije za zavarene konstrukcije – Dimenzije za dužine i uglove – Oblik i položaj.** Beograd, 2024.

[20] Vasilikisa Daniel, Karamanosa Spyros, van Es Sjors, Gresnigt Arnold: **Ultimate bending capacity of spiral-welded steel tubes – Part II: Predictions**. *Thin-Walled Structures,* Vol. 102, 2016, pp. 286–304, http://dx.doi.org/10.1016/j.tws.2015.11.025.

[21] Siemens Digital Industries Software: **FEMAP with NX Nastran, Version 12.0.** Siemens PLM Software, 2018.